ORIGINAL ARTICLE

Cancer Science WILEY

# Tumor-penetrating peptide internalizing RGD enhances radiotherapy efficacy through reducing tumor hypoxia

Fanyan Meng [iD] | Jun Liu | Jia Wei [iD] | Ju Yang [iD] | Chong Zhou | Jing Yan | Baorui Liu [iD]

The Comprehensive Cancer Centre of Nanjing Drum Tower Hospital, The Affiliated Hospital of Nanjing University Medical School, Nanjing, China

**Correspondence**
Baorui Liu, Comprehensive Cancer Centre of Drum Tower Hospital, Medical School of Nanjing University, Clinical Cancer Institute of Nanjing University, 321 Zhongshan Road, Nanjing, 210008, China.
Email: baoruiliu@nju.edu.cn

## Abstract

Resistance to irradiation (IR) remains a major therapeutic challenge in tumor radiotherapy. The development of novel tumor-specific radiosensitizers is crucial for effective radiotherapy against solid tumors. Here, we revealed that remodeling tumor tissue penetration via tumor-penetrating peptide internalizing arginine–glycine–aspartic acid RGD (iRGD) enhanced irradiation efficacy. The growth of 4T1 and CT26 multicellular tumor spheroids (MCTS) and tumors was delayed significantly by the treatment with IR and iRGD. Mechanistically, iRGD reduced hypoxia in MCTS and tumors, resulting in enhanced apoptosis after MCTS and tumors were treated with IR and iRGD. This is the first report that shows enhanced radiation efficacy by remodeling tumor-specific tissue penetration with iRGD, implying the potential clinical application of peptides in future tumor therapy.

**KEYWORDS**
hypoxia, irradiation, multicellular tumor spheroids, radiosensitivity, tumor-penetrating peptides

## 1 | INTRODUCTION

Tumor resistance to irradiation (IR) is still a major challenge that limits the efficacy of radiotherapy. Some drugs and strategies have been designed to enhance the radiosensitivity of solid tumors, however, limited numbers of radiosensitizers are clinically effective against a subset of tumors. One of the major factors limiting the implementation of radiosensitizers in clinical care is poor tumor-specificity.[1] Therefore, the development of novel tumor-specific radiosensitizers remains crucial to enhance radiotherapy efficacy.[2]

Hypoxia is one of the important mechanisms of radiotherapy resistance.[3,4] The response of tumor cells to IR is closely related to the availability of oxygen, and strategies to relieve tumor hypoxia can enhance the efficiency of radiotherapy.[5] Numerous drugs and strategies modifying hypoxia, such as breathing oxygen under normobaric and hyperbaric pressure, blood transfusions, nimorazole administration, and the use of erythropoietin, have been developed and clinically tested[1,6-14]; however, few positive results have shown in the clinical trials.[5,15] Developing novel strategies to reduce hypoxia within tumors is still a great challenge in radiation therapy.

---

----------------------------------------

TPPs are short cyclic peptides that specifically improve the tumor tissue penetration of various drugs, such as chemotherapeutics, contrast agents for MRI, peptides, antibodies, viruses, and nanoparticles.[16-22] They exhibit minimal effects on normal tissues as no significant increase in drug level was observed in other organs or tissues, such as hearts, livers, and lungs.[23,24] After systemic administration, TPPs are initially recruited to tumor blood vessels and tumor tissues by binding to the primary endothelial receptors, then proteolytic cleaved to the C-end rule (CendR) motifs (R/KXXR/K). The CendR motifs bind to NRP-1 and activate the penetration pathway through tumor tissues.[25]

In this study, we revealed that internalizing RGD (iRGD), a tumor-penetrating peptide, enhances the radiosensitivity of 4T1 and CT26 multicellular tumor spheroids and tumors by reducing hypoxia. Our work provides a novel and effective tumor-specific strategy to enhance the therapeutic efficacy of IR, implying the potential clinical application of TPPs in future IR-based tumor therapy.

# 2 | MATERIALS AND METHODS

## 2.1 | Peptides

Peptides iRGD (cyclic CRGDKGPDC), RGD (cyclic CRGDDGPKC) and RGE (cyclic CRGEKGPDC) were synthesized using ChinaPeptides Co., Ltd. The purity of all peptides was ~98%.

## 2.2 | Animals and cell lines

Mouse breast cancer cell line 4T1 was obtained from the American Type Culture Collection (ATCC). Mouse colon cancer cell line CT26 was obtained from the Cell Bank of the Chinese Academy of Sciences. Cell lines 4T1 and CT26 are often used in studies on TPPs, hypoxia, and radiation.[26-29] Cells were cultured in RPMI 1640 medium supplemented with 10% FBS and antibiotics (100 U/mL penicillin and 100 μg/mL streptomycin). Six- to 8-week-old female BALB/c mice were obtained from the Animal Core Facility of Nanjing Medical University, Nanjing, China for use in these experiments. Mouse studies were approved by the Laboratory Animal Care and Use Committee of the Affiliated Nanjing Drum Tower Hospital of Nanjing University Medical School.

## 2.3 | Cell proliferation

For cell proliferation assay, 4T1 cells were seeded into 96-well plates ($10^3$ cells/well) and incubated overnight at 37°C and 5% $CO_2$. Peptide iRGD was added into the medium at 95 μg/mL (100 μM), according to the published procedures.[30,31] After 4 h, cells were irradiated to 5, 10, or 20 Gy. Cell proliferation was measured using the Cell Counting Kit-8 (CCK-8, KeyGen BioTECH) every other day according to the manufacturer's instructions. Cells were incubated with CCK-8 for 4 h, and then the optical density at 450 nm (OD450) was measured using a microplate reader Infinite F Plex (TECAN).

## 2.4 | Multicellular tumor spheroid (MCTS) growth curves

Multicellular tumor spheroids were initiated by inoculating 2000 cells in 100 μl growth medium per well into 96-well round-bottomed ultra-low attachment microplates (Corning). At 48 h later, iRGD were added into wells and radiation with the indicated dose was performed after MCTS were cultured with peptides for 4 h. The final concentration of iRGD is 25 μg/mL, except for other concentrations described in some assays. Diameters of the MCTS were measured using ImageJ software every other day. The volume of a spheroid was calculated in accordance with the formula $V = (1/6)\pi d^3$, where d = diameter.

## 2.5 | Clonogenic survival assay

Clonogenic survival assay was performed as previously described.[30] Briefly, MCTS were treated with peptides and radiation. Spheroids were dissociated into single cells by trypsinization. Cells from spheroids were plated into 6-well plates at 2000 cells per well and incubated at 37°C in an humidified incubator. At 7 days later, colonies were fixed in 4% paraformaldehyde and stained with 1% crystal violet. Colonies containing more than 50 cells were scored. For dose–cell survival assay, curves were fitted with a single-hit multitarget model using GraphPad Prism 8 software. For the clonogenic survival assay on high-density cultured cells, $5 \times 10^4$ cells per well were seeded into the 24-well plates. At 24 h later, the cells were radiated with the indicated doses. After another 24 h, cells were trypsinized and seeded into 6-well plates. At 10 days later, the cells were stained with crystal violet and counted.

## 2.6 | Cell migration assay

Multicellular tumor spheroids were cultured for 2 days and treated with peptides and radiation. Spheroids were dissociated into single cells by trypsinization. Cells from spheroids were plated in Millicell Cell Culture Inserts at 500 cells per well and incubated at 37°C in a humidified incubator. At 24 h later, inner cells were removed and migrated cells were fixed in 4% paraformaldehyde and stained with 1% crystal violet.

## 2.7 | Quantitative polymerase chain reaction (Q-PCR)

Multicellular tumor spheroids were treated with peptides for 6 h and harvested to tubes. RNA was extracted with TRIzol reagent

(Thermo Fisher Scientific, 15596018). Reverse transcription were performed using the Transcriptor First Strand cDNA Synthesis Kit (Roche, 04897030001). Q-PCR was performed with the kit and analyzed using SYBR® Select Master Mix (Thermo Fisher Scientific Inc., 4472908). Primers are listed in Table S1.

## 2.8 | *In vivo* anti-tumor effect and side effects study

The 4T1 tumor cells ($5 \times 10^4$) were injected into the mammary gland of female BALB/c mice. The CT26 tumor cells ($2 \times 10^5$) were injected subcutaneously into the right flank of male BALB/c mice. At 11 days later after tumor cell injection, peptide (iRGD, RGD or RGE) was administered into mice via intravenous (iv) or intraperitoneal (ip) injection. At 4 h later, the mice were anesthetized and tumors were locally irradiated with 5 Gy using the electron linear accelerator. All of the mice were observed daily and the body weight and tumor volume (by a digital Vernier caliper) were measured every other day. Mice were sacrificed at the end of the experiment. Both tumor tissues and main organs (heart, liver, spleen, lung and kidney) were dissected for histology observation. Tumor volume was calculated using the formula for approximating the volume of a spheroid (width × width × length/2). H&E staining of paraffin-embedded lung tissue was performed for histological examination of metastases. Sections were examined on a Primovert microscope (Carl Zeiss AG). The surface area of metastatic lesions was analyzed using ImageJ software (National Institutes of Health). Metastatic tumor area was calculated as a percentage of metastatic area as a whole by dividing by the entire area of lung tissue.

## 2.9 | Immunofluorescence

Peptides were injected iv into 4T1 tumor-bearing mice and pimonidazole hydrochloride (60 mg/kg; Hypoxyprobe Inc., HP1-100Kit) was administered into mice via iv injection. Pimonidazole is a non-toxic 2-nitroimidazole compound that binds thiol groups to proteins, peptides, and amino acids in hypoxic regions, and could be used as an effective exogenous hypoxia probe.[31] Tumors were surgically excised at 1 h after pimonidazole hydrochloride injection. Tumor tissues were paraffin embedded, sectioned, and stained with FITC-conjugated mouse anti-pimonidazole protein adducts antibody (Hypoxyprobe Inc., HP1-100 Kit; 1:100) and goat anti-mouse CD31 antibody (Servicebio, GB13063; 1:100). Cy3-conjugated donkey anti-goat IgG (Servicebio, GB21404; 1:100) was used as a secondary antibody to stain CD31. The tissue samples on slides were mounted with ProLong™ Gold Antifade Mountant with DAPI (Thermo Fisher Scientific, P36935).

### 2.9.1 | Apoptosis analysis

For detecting apoptosis in MCTS, spheroids were treated with peptides and radiation. MCTS were harvested after treatment for 48 h.

Single cells were prepared by trypsinization and stained with fluorescein isothiocyanate (FITC)-conjugated anti-annexin V antibody and PI (MultiSciences, 70-AP101-100). Early apoptotic cells are annexin V-positive and PI-negative (FITC$^+$/PI$^-$), whereas late apoptotic and dead cells are annexin V-positive and PI-positive (FITC$^+$/PI$^+$). For detecting apoptosis in tumor tissues, tumor-bearing mice were treated with peptides for 4 h and then received radiation. At 24 h later, tumors were surgically excised. Tumor tissues were paraffin embedded, sectioned, and stained using the TACS® 2 TdT-Fluor In Situ Apoptosis Detection Kit (Trevigen Inc., 4812-30-K), which was based on the TUNEL assay.

### 2.9.2 | Flow cytometry

Hypoxia of MCTS was evaluated using the Hypoxyprobe™-1 Kit. Spheroids were treated with peptides and cultured for 0, 2, 4, 6, and 9 h, separately. Pimonidazole hydrochloride was added into wells containing MCTS and incubated for 40 min. Single cells were prepared by trypsinization and washed with PBS containing 1% FBS. Cells were stained with FITC-conjugated mouse monoclonal antibody directed against pimonidazole protein adducts (Hypoxyprobe Inc., HP1-100Kit) and analyzed using a BD Accuri C6 flow cytometer (Becton, Dickinson and Company). Samples were collected on a BD Accuri C6 flow cytometer, and data were analyzed using FlowJo software (Tree Star Inc.).

### 2.9.3 | Statistical analysis

All values were presented as mean ± SD. Two-tailed unpaired Student *t*-tests were used for comparisons between two groups. Two-way ANOVA was used for the growth curve comparison. A *p*-value of <0.05 was considered statistically significant. For all tests, symbols represent the following: *$p < 0.05$; **$p < 0.01$; ***$p < 0.001$. ns means not significant.

## 3 | RESULTS

### 3.1 | Tumor-penetrating peptide iRGD improved the efficacy of IR on multicellular tumor spheroids

We aimed to look for new radiosensitizers with a higher tumor-specificity and found occasionally that iRGD could enhance the efficacy of IR on MCTS after the technique of iRGD-modified T-cell immunotherapy was established by our group.[32] Mouse breast cancer 4T1 cells cultured as MCTS were treated with 95 μg/mL iRGD, followed by 2 or 5 Gy IR (Figure 1A). Two 9-amino acid cyclic peptides, RGD and RGE, were used as the control peptides in this study. The RGD peptide contains an arginine–glycine–aspartic acid (RGD) motif, but lacks a cryptic CendR motif, resulting in a tumor-targeting property without tissue penetration. The RGE

peptide contains a mutant amino acid in the RGD motif, resulting in a loss of the tumor-targeting property. We found that the growth of MCTS was greatly hindered by IR with iRGD compared with the growth of MCTS that received IR alone. Without IR, cell growth did not change significantly when MCTS were treated with iRGD. In contrast with iRGD, treatment with the two control peptides RGD and RGE did not significantly affect the growth of irradiated MCTS (Figures 1B and S1). When the concentration of iRGD was increased from 0.2 to 12.5 μg/mL, the growth rate of MCTS decreased gradually (Figure 1C). The effects of iRGD on IR were also confirmed by clonogenic survival assays. The colony area and numbers were noticeably reduced when MCTS were treated with

2 Gy radiation and iRGD (Figures 1D,E and S2). The migration ability of 4T1 cells in MCTS was also repressed after treatment with IR and iRGD. The numbers of migrated tumor cells in the group treated with radiation and iRGD decreased to 42% compared with the group treated with radiation alone. Treatment with peptides RGD and RGE did not have significant effects on radiated cells in the migration assay (Figure 1F), suggesting that both the tumor targeting and the CendR motifs are important for iRGD-enhanced IR efficacy. Another cell line, mouse colon carcinoma CT26, was also tested. The growth of MCTS of CT26 was greatly hindered by IR with iRGD compared with the growth of MCTS that received IR alone (Figure 1G).
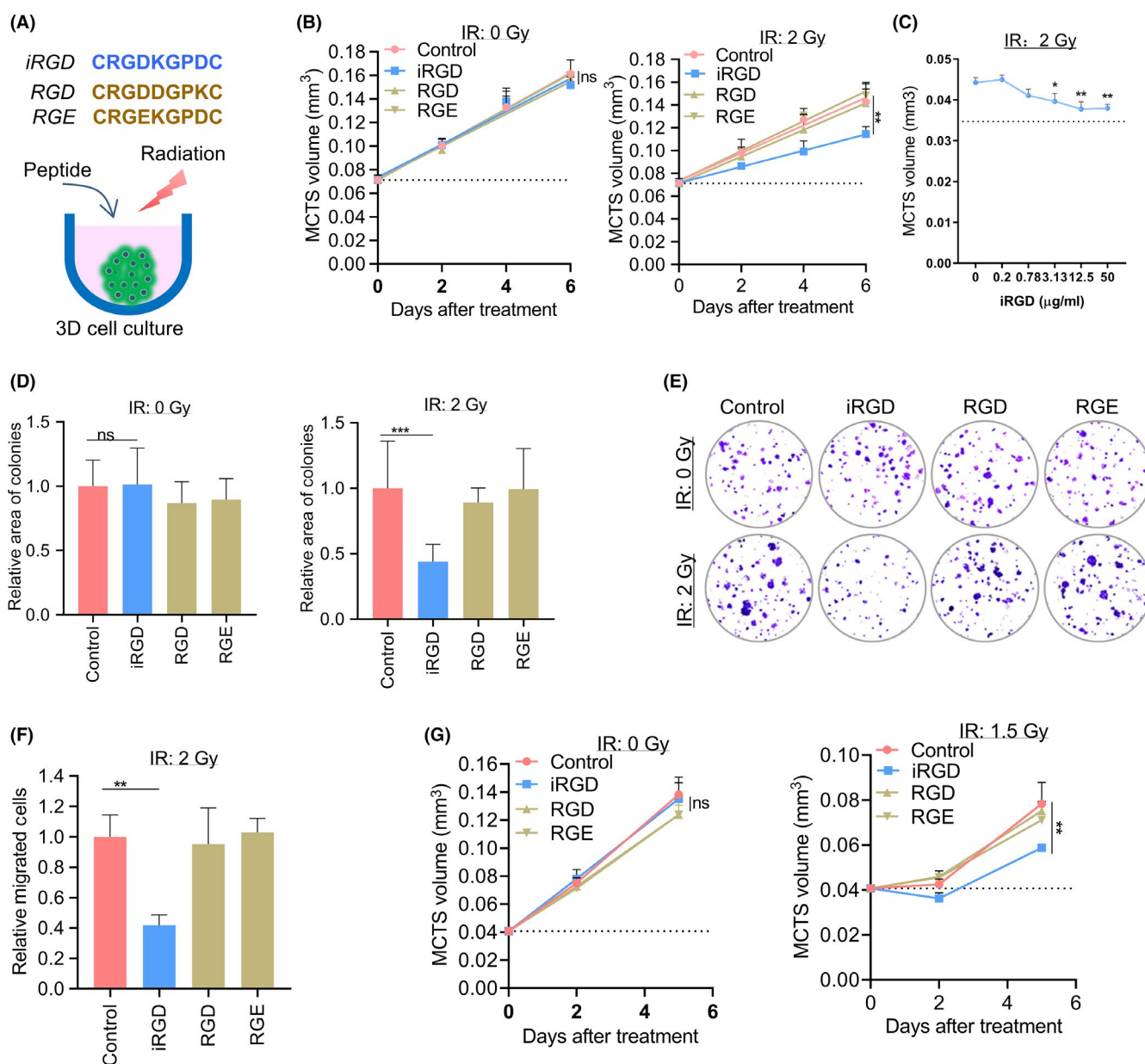


**FIGURE 1** Tumor-penetrating peptide iRGD enhanced the efficacy of radiation therapy *in vitro*. (A) Model of the treatment with iRGD and IR. (B) Growth curves of MCTS treated with 2 Gy radiation and peptides. (C) Growth of MCTS treated with various concentrations of iRGD peptide. (D) Relative area of colonies formed under different treatments. (E) Representative pictures of colonies. (F) Migrated cells under different treatments. (G) Growth curves of CT26 MCTS treated with iRGD and control peptides with or without 1.5 Gy IR

## 3.2 | iRGD-enhanced anti-tumor efficacy of irradiation *in vivo*

To evaluate the effect of iRGD on the efficacy of IR for inhibiting tumor growth, 4T1 cells were injected into the mammary glands of female BALB/C mice. At 11 days after the injection of tumor cells, iRGD was administered to the mice via intravenous injection. Tumors were locally irradiated with a dose of 5 Gy after peptide injection (Figure 2A). The 4T1 tumor-bearing mice treated with combined IR and iRGD showed significantly inhibited tumor growth compared with the control group that was treated with PBS. In contrast, single treatment with iRGD or 5 Gy IR had no significant effect on the growth of 4T1 tumors (Figure 2B). Consistent with the results of tumor growth, the tumor burden of the group treated with the combined IR and iRGD decreased significantly compared with the control group and the groups that received a single treatment of IR or iRGD. In fact, the average tumor weight of the combined treatment group decreased to 40% of the controls (Figure 2C). We also tested the effect of iRGD via ip injection. Tumor growth in the group treated with the combination of IR and iRGD was also significantly suppressed compared with that of the control group (Figure S3). Furthermore, we estimated the effect of iRGD and IR

treatment on tumor distal metastasis. Metastatic lesions in the lung in the combined treatment group decreased significantly compared with those of the control group and with the groups that received single treatment of IR or iRGD. The average tumor metastasis of the combined treatment group was reduced by 50% compared with that of the control group (Figures 2D and S4). The tumor growth and tumor weight of groups treated with the combined treatment of IR and RGD or RGE showed no significant changes compared with the control group (Figure S5).

CT26 tumor models were also evaluated with the same procedures as 4T1. We observed that the CT26 tumor growth and tumor weight in the group treated with the combination of IR and iRGD was also significantly suppressed compared with that of the control group (Figure 2E–G).

None of the mice treated with IR and iRGD showed any body weight loss compared with the control group (Figure 3). To assess the potential toxicity of single and combination treatment in mice, H&E-stained heart, liver, and kidney sections were examined. There were no obvious additional pathologic changes in these organs in the group treated with IR and iRGD, compared with that in groups given single treatments of IR, iRGD or PBS controls (Figure S6).
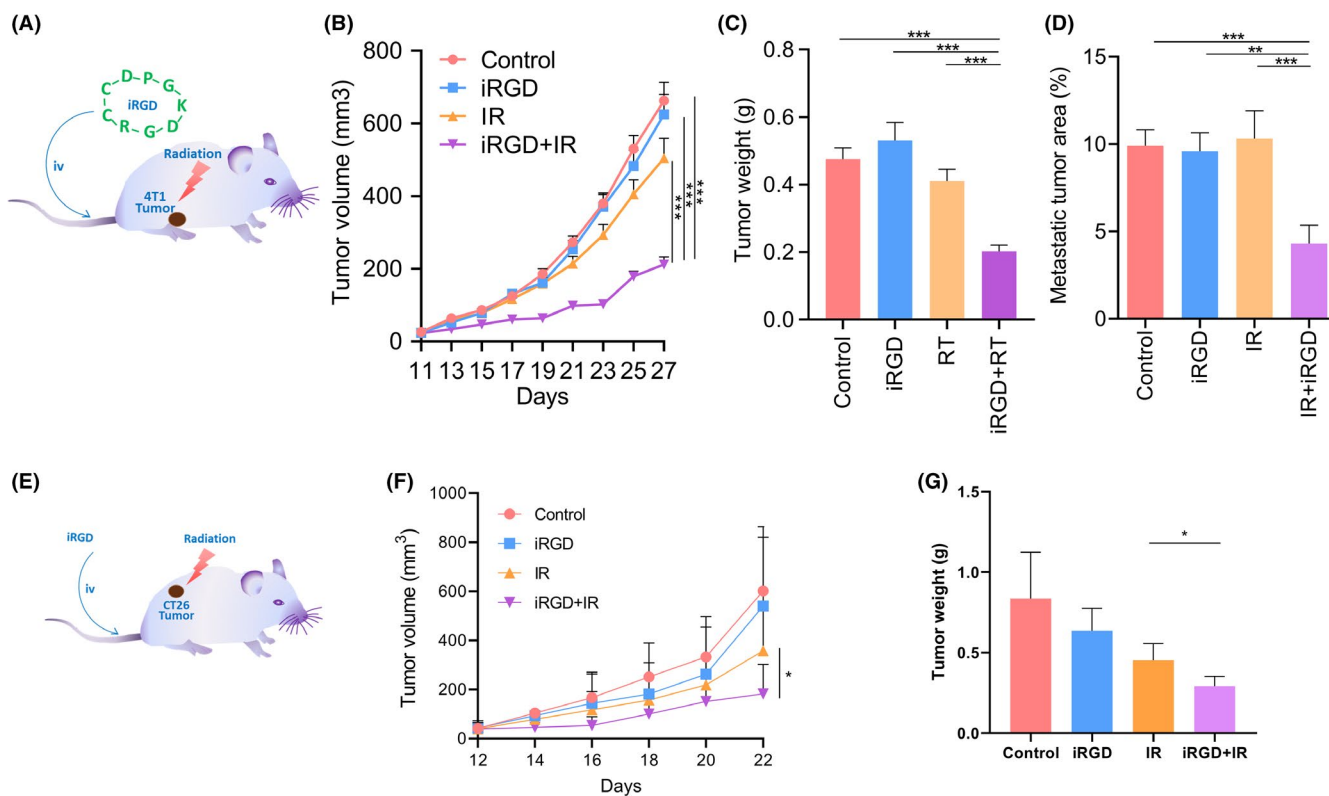


**FIGURE 2** Tumor-penetrating peptide iRGD enhanced the efficacy of radiation therapy *in vivo*. (A, E) Schematic description of tumor-penetrating peptide iRGD combined with radiation treatment. (B) Combination therapy with IR and iRGD greatly delayed 4T1 tumor growth compared with single treatments. (C) Combination therapy greatly inhibited 4T1 tumor weight compared with single treatments. (D) Combination therapy dramatically reduced lung metastasis compared with single treatments. Metastatic tumor area was quantified by the percentage of metastatic area relative to total lung area. (F) Combination therapy greatly delayed CT26 tumor growth compared with IR treatment alone. (G) Combination therapy greatly reduced CT26 tumor weight compared with IR treatment alone

IR at 5 Gy combined with iRGD treatment significantly inhibited tumor growth and metastasis *in vivo*, and exhibited the approximate therapeutic efficiency at high dose of IR of 15 Gy (Figure S7A,B). However, treatment with IR at 15 Gy resulted in the marked reduction in mouse body weight (Figure S7C). In contrast, the body weight of mice in the group treated with IR at 5 Gy and iRGD did not change significantly compared with the control group, suggesting that treatment with IR and iRGD produced good safety.
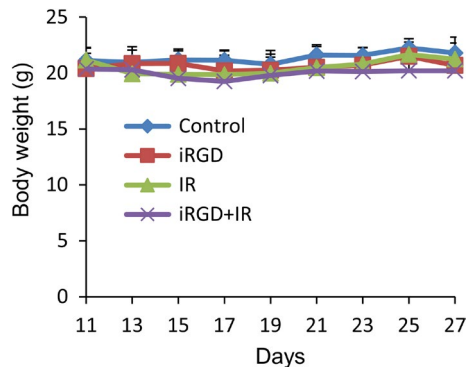
### 3.3 | IRGD increased the apoptosis in MCTS and tumor tissues induced by IR

Next, we investigated whether IR combined with iRGD promoted apoptosis at the cellular level. (Figure 4A). The percentages of early apoptosis, late apoptosis, and dead cells, along with total apoptosis, increased significantly in groups treated with IR with iRGD, compared with the IR alone group or in the IR with control peptide group (Figure 4B–E). No significant difference was observed among the groups treated with peptides alone (Figure S8).

Consistent with the aforementioned results on MCTS, the apoptosis index of tumor tissues after IR treatment in the iRGD groups were also increased significantly (Figure 5A,B).

### 3.4 | IRGD reduced hypoxia of MCTS

We next determined the mechanisms involved in enhancement of radiotherapy efficacy by iRGD. We first tested the effects of IR and iRGD on low-density monolayer cells. As shown in Figure S9, iRGD did not impact the growth of 4T1 cells cultured in two-dimensional (2D) monolayer cell culture upon radiation (2 or 5 Gy), suggesting that iRGD did not affect tumor cell radiosensitivity directly. Then
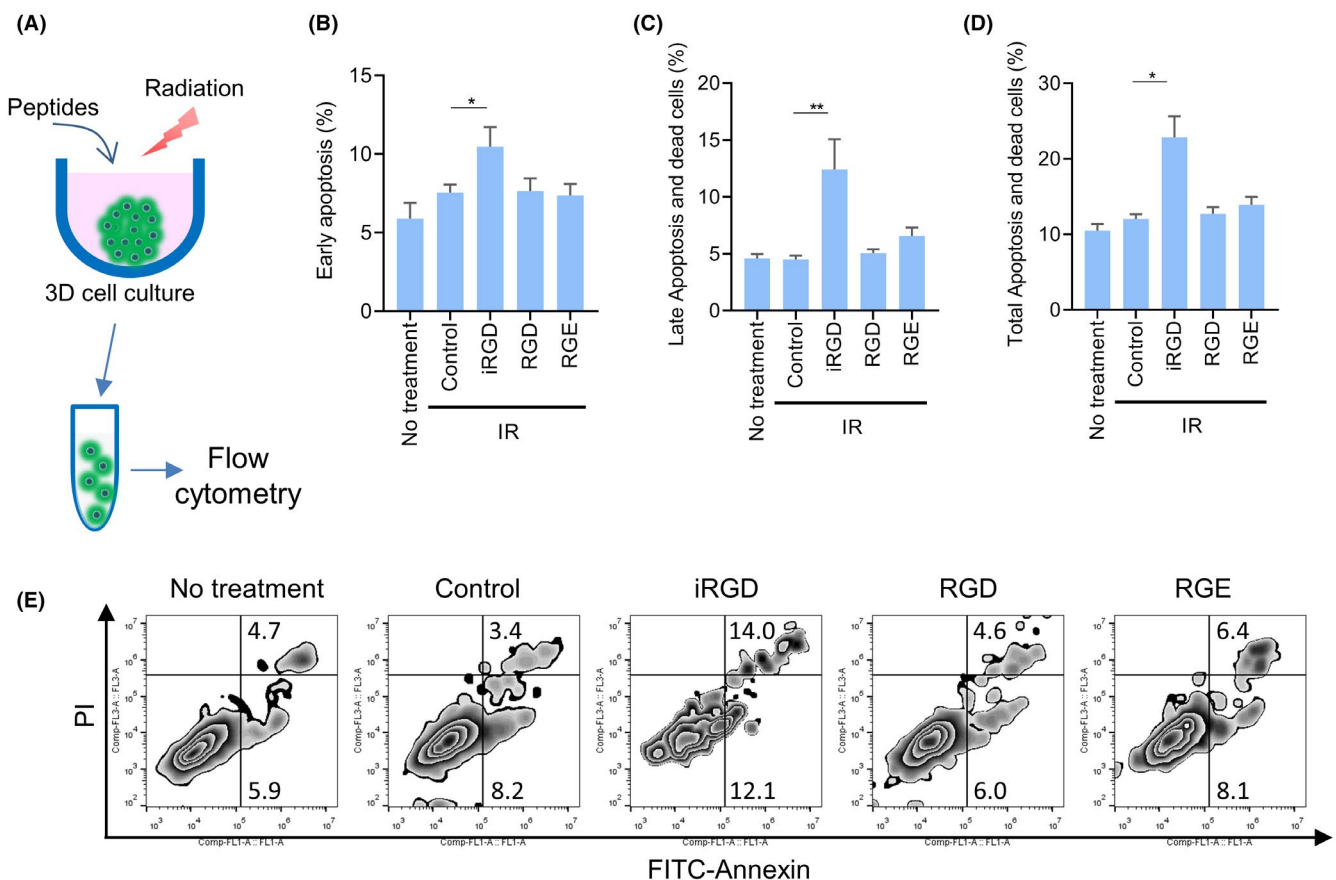


**FIGURE 3** Body weight change of 4T1 tumor-bearing mice that received the iRGD and IR treatment



**FIGURE 4** Tumor-penetrating peptide iRGD promoted IR-induced apoptosis *in vitro*. (A) Model for treatments of MCTS. (B–D) Percentages of early apoptosis (B), late apoptosis and dead (C) and total apoptosis (D) cells in MCTS treated with IR and peptides. (E) Representative scatterplots of annexin V/PI staining
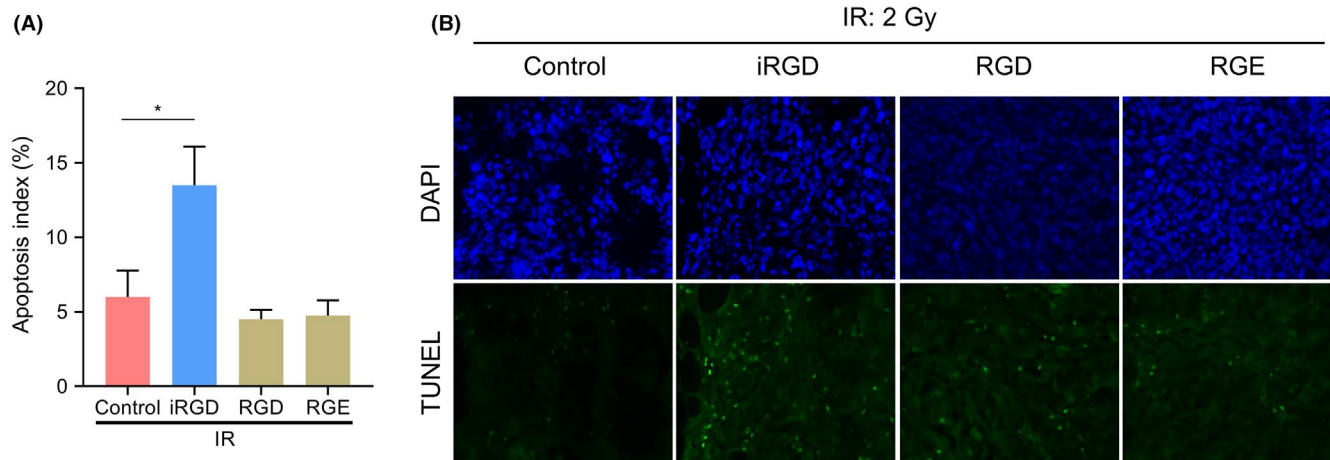
**(A)**



**(B)**

IR: 2 Gy



**FIGURE 5** Tumor-penetrating peptide iRGD promoted IR-induced apoptosis *in vivo*. (A) Percentages of apoptotic cells in tumor tissues treated with IR and peptides. (B) Representative TUNEL immunofluorescence of the tumor tissues

**FIGURE 6** Tumor-penetrating peptide iRGD reduced hypoxia in MCTS. (A) Schematic description of three-dimensional (3D) MCTS culture. (B) Representative immunofluorescence of MCTS stained with anti-pimo (green) antibody and DAPI (blue). (C) Relative hypoxic cells (pimo$^+$) in MCTS after administration of iRGD for the indicated times. (D) Relative hypoxic cells (pimo$^+$) in MCTS after administration of peptides for 4 h. (E) Percentages of hypoxic cells (pimo$^+$) in MCTS under different treatments. (F) Relative mRNA expression of four hypoxia-related genes in MCTS under different treatments
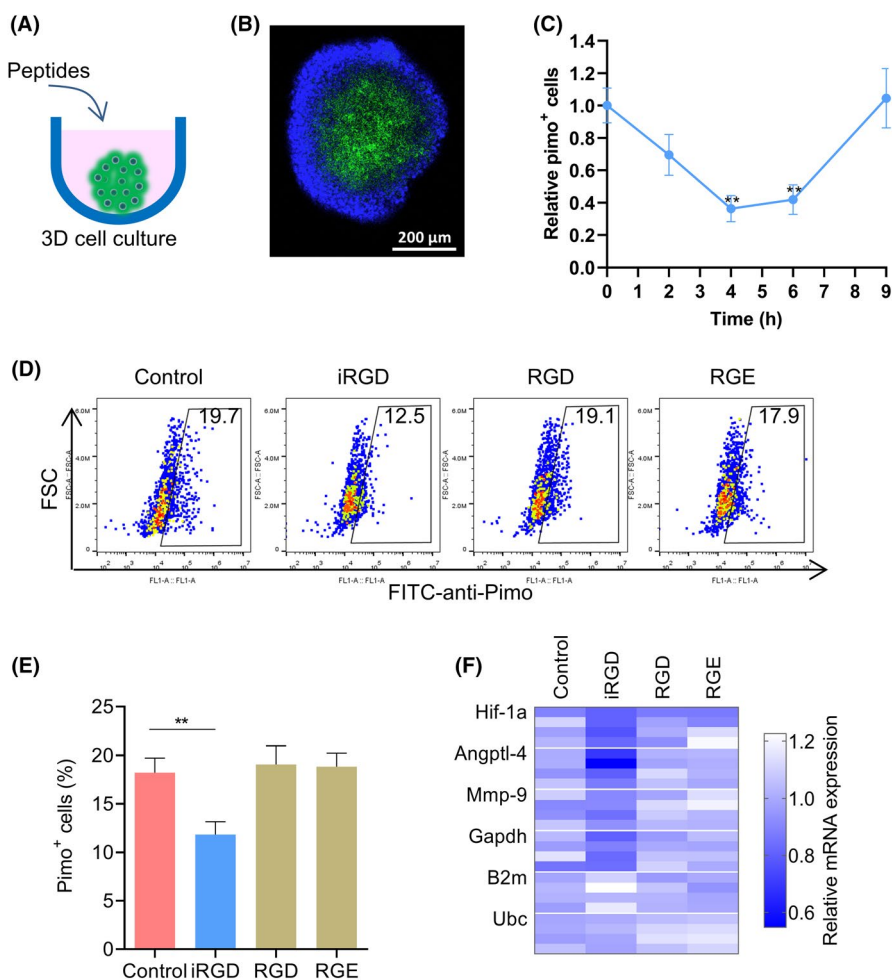


we tested the effects of IR and iRGD on high-density monolayer cells with a radioresistant cell-contact effect, which may be involved in MCTS radioresistance.[33] However, iRGD did not influence the growth of 4T1 cells cultured in high-density monolayer cell culture upon radiation (Figure S10). Consistent with the above results, no difference in apoptosis was observed among the IR and peptide-treated groups when 4T1 tumor cells were cultured in a 2D

monolayer system without hypoxia at the low (Figure S11) and high (Figure S12) cell densities.

At MCTS have three-dimensional structures with hypoxic areas inside, we wanted to find out whether iRGD increased cell radiotherapy sensitivity by affecting hypoxia. IRGD can promote small molecules to penetrate deeply into tumor tissues.[34] Oxygen molecules and doxorubicin have similar properties in the way they enter

the cell or tissue through passive diffusion. So, we wanted to verify if iRGD could promote oxygen molecules to penetrate into MCTS and tumor tissues and alleviate hypoxia. MCTS of 4T1 were treated with iRGD for various durations. Hypoxia of MCTS were detected with the Hypoxyprob-1 kit based on pimonidazole (Figure 6A). Tumor spheroids contained a normoxic outer shell and a hypoxic core (Figure 6B), as reported elsewhere.[35] The relative percentages of pimonidazole adducts (pimo) positive cells in the MCTS group with iRGD treatment declined to ~50% after treatment for 4 and 6 h, and recovered to the baseline after 9 h (Figure 6C). The percentages in groups treated with RGD or RGE for 4 h did not change significantly, although the relative percentages of pimo positive cells in the iRGD-treated MCTS group declined at this time point (Figure 6D,E). Hypoxia was also evaluated by measuring the mRNA levels of hypoxia-related genes, with *Actb* as a reference gene. The mRNA expression of four hypoxia-related genes *Hif-1a*, *Angptl-4*, *Mmp-9*, and *Gapdh* in groups treated with iRGD declined compared with that in the PBS control group (Figure 6F). Two frequently used housekeeping genes *B2m* and *Ubc* showed relatively stable expression patterns in all the groups.

Single-hit multitarget mathematical models are widely used to explain the radiation killing of cells.[36] Dose–cell survival curves fitted with a single-hit multitarget model demonstrated the consistent results with hypoxia reduction (Figure S13). Cells in MCTS treated with iRGD showed the lower values of mean lethal dose D0 (10.85 vs. 14.07), the quasithreshold dose Dq (1.73 vs. 7.69), and the extrapolation number N (1.17 vs. 1.73) in contrast with that of the control group treated with PBS, suggesting that hypoxia reduction did contribute to cell sensitivity to IR.

## 3.5 | IRGD reduced tumor *tissue* hypoxia

Hypoxia is a common characteristic of solid tumors, even at an early stage of tumor development (in <5 mm$^3$ tumors).[37] Hypoxia in tumor tissues treated with different peptides was evaluated by pimonidazole adduct staining (Figure 7A). The percentages of hypoxic area in iRGD-treated groups reduced significantly, compared with

that of the control group. In contrast, the percentages of hypoxic area in RGD- or RGE-treated groups did not change significantly (Figure 7B,C).

## 3.6 | Neuropilin-1 (NRP-1) is the critical molecules for iRGD to reduce hypoxia and to enhance the efficacy of IR

Finally, we sought to reveal whether iRGD reduced hypoxia and enhanced the efficacy of IR through NRP-1. Cyclic peptide iRGD can bind to $\alpha_V\beta_3/\beta_5$ integrins and NRP-1.[38] Truncated iRGD (t-iRGD, CRGDK) loses much of its affinity for integrin, but possesses the affinity for NRP-1.[39] The percentage of hypoxic cells in MCTS decreased greatly when MCTS were treated with t-iRGD, suggesting that NRP-1 may mediate hypoxia reduction (Figure 8A). Hypoxia reduction of iRGD vanished when NRP-1 was blocked with anti-NRP-1 blocking antibody (Figure 8B). At the same time, MCTS growth inhibition of IR combined with iRGD also disappeared after NRP-1 blocking (Figure 8C). The above results demonstrated that NRP-1 is the critical molecule for iRGD to reduce hypoxia and to enhance the efficacy of IR.

## 4 | DISCUSSION

Peptide iRGD can increase tumor tissue penetration and enhance the accumulation in tumors of various drugs such as chemotherapeutics, contrast agents for MRI, peptides and recombinant proteins, antibodies, viruses, and nanoparticles. In this study, we demonstrated that iRGD also enhanced the efficacy of radiation therapy. IR at 5 Gy combined with iRGD treatment significantly suppressed 4T1 tumor growth and metastasis *in vivo*, with the same therapeutic efficiency at a high dose of IR of 15 Gy alone. The body weight of mice in the group treated with IR at 5 Gy and iRGD did not change significantly compared with the control group. There were no obvious additional pathologic changes in these organs in the group treated with IR and iRGD, suggesting that treatment
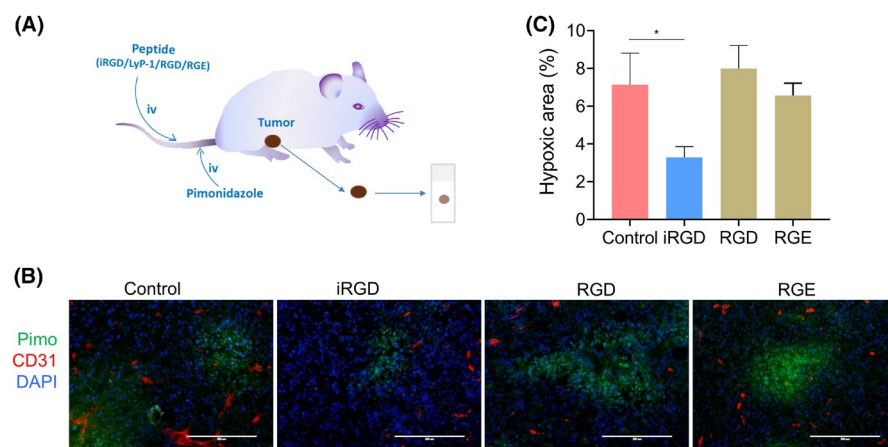


**FIGURE 7** Tumor-penetrating peptide iRGD reduced tumor hypoxia *in vivo*. (A) Model for tumor hypoxia detection. (B) Representative immunofluorescence of the tumor tissues stained with anti-pimo (green), anti-mouse CD31 (red) and DAPI (blue) (C) Percentages of hypoxic area (pimo$^+$) in tumors treated with iRGD and control peptides

with IR and iRGD produced good safety. However, more toxicological studies should be performed before clinical trials are initiated. Peptide iRGD can reverse tumor hypoxia, but there may be a risk of the overgrowth of re-oxygenated tumor cells. Timely and effective radiotherapy must be applied to reduce the risk of re-oxygenated tumor cell growth.

Tumor growth did not change significantly when iRGD alone was administrated to mice via iv or ip injection in our study, which is consistent with other reports.[16,23] One study reported that tumor-penetrating peptide iRGD inhibited metastasis when iRGD was iv injected every other day into nude mice with orthotopic human prostate and pancreatic tumors.[40] There were no significant differences in lung metastasis among groups treated with or without iRGD in the absence of IR in our study. In fact, another report showed that tumor metastasis in mice injected with a single intravenous dose of iRGD was not statistically different from that in the vehicle control.[41] Results from these studies indicated that the effects of iRGD on tumor metastasis are multiple and may vary depending on tumor types, mouse models, and the administrated strategies of peptides adopted in the studies.

Peptide iRGD reduced hypoxia and enhanced the efficacy of IR through NRP-1. Peptide iRGD binds to $\alpha v\beta 3/\alpha v\beta 5$ integrins and is cleaved by proteases to generate a CendR–containing fragment. Then CendR sequence binds to NRP-1 and activates the bulk transport endocytosis pathway, which is different from known endocytic processes and partially characterized now.[42] It was demonstrated that NRP1-GAIP interacting protein C terminus, member 1 (GIPC1)/synectin interaction plays an important role in the initial internalization, and the penetration pathway is regulated by mTOR signaling. Oxygen molecules and some small molecule drugs, such as doxorubicin and paclitaxel, share similar properties in the way they enter cells or tissues through passive diffusion. Based on the existing knowledge, we speculated that oxygen molecules pass deeply into tumor tissues through the NRP1-mediated endocytosis pathway. Further studies should be performed to verify the detailed mechanisms involved in oxygen transport into tumor tissue in the context of iRGD administration in the future.

Collectively, these data supported the hypothesis that improving tumor-specific tissue penetration using iRGD-enhanced efficacy of IR by reducing tumor hypoxia (Figure 8D). One of the strengths of iRGD is to enhance tissue penetration, which is highly tumor specific. IRGD contains three independent modules: a vascular homing motif, a CendR tissue penetration motif, and a protease recognition site. These modules cooperate to ensure a high specificity of tumor targeting and penetration.[25] In contrast, other strategies to overcome hypoxia, such as hyperbaric oxygen inhalation, red blood cell transfusion, erythropoietin injection, oxygen mimics and hypoxic cytotoxins, are not tumor specific and result in confused clinical
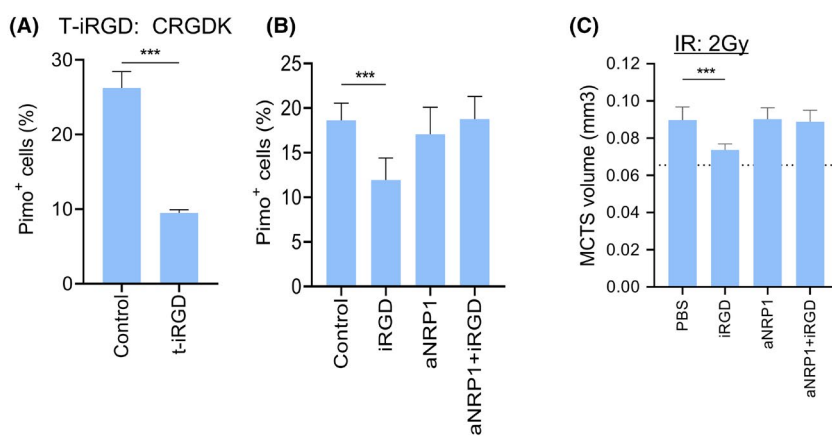


**FIGURE 8** NRP-1 is the critical molecules for iRGD to reduce hypoxia and to enhance the efficacy of IR. (A) Hypoxic cell percentages of MCTS treated with t-iRGD or PBS. (B) Relative hypoxic cells in MCTS treated with iRGD after NRP-1 blocking. (C) Growth of MCTS treated with iRGD after NRP-1 blocking. (D) Mechanistic model of the enhancement of IR efficacy by iRGD. Tumor-penetrating peptide iRGD increases the penetration of molecular oxygen and reduce hypoxia in MCTS and tumors through NRP-1 pathway, leading to increased sensitivity of tumor cells to IR. As a result, the apoptosis of tumor cells increased and tumor burden and metastasis decreased
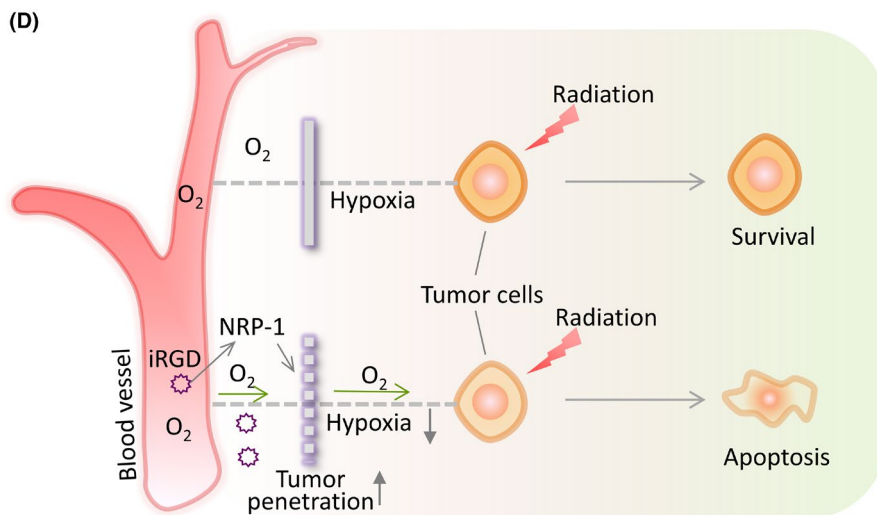
outcomes.[1,43] Moreover, iRGD showed a versatile ability to facilitate the penetration of therapeutic drugs into tumors, enhancing the efficacy of IR. Thereby, iRGD appeared to exhibit great potential in the combination of radiotherapy with chemotherapy or immunotherapy. Last, considering that receptors of iRGD are universally expressed in various tumors, this novel and effective strategy of IR-based therapy has great potential for clinic use in the future after rigorous and detailed clinical studies.

## ACKNOWLEDGMENTS

## CONFLICTS OF INTEREST

The authors have declared that no conflict of interest exists.

## ORCID

*Fanyan Meng* https://orcid.org/0000-0003-1187-7644
*Jia Wei* https://orcid.org/0000-0003-3024-8878
*Ju Yang* https://orcid.org/0000-0001-5305-7893
*Baorui Liu* https://orcid.org/0000-0002-2539-7732

## REFERENCES

1. Moding EJ, Kastan MB, Kirsch DG. Strategies for optimizing the response of cancer and normal tissues to radiation. *Nat Rev Drug Discov*. 2013;12:526-542.
2. Tu X, Kahila MM, Zhou Q, et al. ATR inhibition is a promising radiosensitizing strategy for triple-negative breast cancer. *Mol Cancer Ther*. 2018;17:2462-2472.
3. Graham K, Unger E. Overcoming tumor hypoxia as a barrier to radiotherapy, chemotherapy and immunotherapy in cancer treatment. *Int J Nanomedicine*. 2018;13:6049-6058.
4. Carlson DJ, Yenice KM, Orton CG. Tumor hypoxia is an important mechanism of radioresistance in hypofractionated radiotherapy and must be considered in the treatment planning process. *Med Phys*. 2011;38:6347-6350.
5. Benej M, Hong X, Vibhute S, et al. Papaverine and its derivatives radiosensitize solid tumors by inhibiting mitochondrial metabolism. *Proc Natl Acad Sci USA*. 2018;115:E11561.
6. Pinel S, Barberi-Heyob M, Cohen-Jonathan E, et al. Erythropoietin-induced reduction of hypoxia before and during fractionated irradiation contributes to improvement of radioresponse in human glioma xenografts. *Int J Radiat Oncol Biol Phys*. 2004;59:250-259.
7. Hirst DG. Oxygen delivery to tumors. *Int J Radiat Oncol Biol Phys*. 1986;12:1271-1277.
8. De Ridder M, Van Esch G, Engels B, Verovski V, Storme G. Hypoxic tumor cell radiosensitization: role of the iNOS/NO pathway. *Bull Cancer*. 2008;95:282-291.
9. Welsh L, Panek R, Riddell A, et al. Blood transfusion during radical chemo-radiotherapy does not reduce tumour hypoxia in squamous cell cancer of the head and neck. *Br J Cancer*. 2017;116:28-35.
10. Poskitt TR. Radiation therapy and the role of red blood cell transfusion. *Cancer Invest*. 1987;5:231-236.
11. Ang KK. More lessons learned from the suffocation of hypoxia. *J Clin Oncol*. 2010;28:2941-2943.
12. Tharmalingham H, Hoskin P. Clinical trials targeting hypoxia. *Br J Radiol*. 2019;92(1093):20170966.
13. Hassan Metwally MA, Ali R, Kuddu M, et al. IAEA-HypoX. A randomized multicenter study of the hypoxic radiosensitizer nimorazole concomitant with accelerated radiotherapy in head and neck squamous cell carcinoma. *Radiother Oncol*. 2015;116:15-20.
14. Thomson D, Yang H, Baines H, et al. NIMRAD – a phase III trial to investigate the use of nimorazole hypoxia modification with intensity-modulated radiotherapy in head and neck cancer. *Clin Oncol*. 2014;26:344-347.
15. Chen HHW, Kuo MT. Improving radiotherapy in cancer treatment: Promises and challenges. *Oncotarget*. 2017;8:62742-62758.
16. Sugahara KN, Teesalu T, Karmali PP, et al. Tissue-penetrating delivery of compounds and nanoparticles into tumors. *Cancer Cell*. 2009;16:510-520.
17. Puig-Saus C, Rojas LA, Laborda E, et al. iRGD tumor-penetrating peptide-modified oncolytic adenovirus shows enhanced tumor transduction, intratumoral dissemination and antitumor efficacy. *Gene Ther*. 2014;21:767-774.
18. Xin X, Sha H, Shen J, Zhang B, Zhu B, Liu B. Coupling GdDTPA with a bispecific, recombinant protein antiEGFRiRGD complex improves tumor targeting in MRI. *Oncol Rep*. 2016;35:3227-3235.
19. Huang Y, Li X, Sha H, et al. Tumor-penetrating peptide fused to a pro-apoptotic peptide facilitates effective gastric cancer therapy. *Oncol Rep*. 2017;37:2063-2070.
20. Liu X, Lin P, Perrett I, et al. Tumor-penetrating peptide enhances transcytosis of silicasome-based chemotherapy for pancreatic cancer. *J Clin Invest*. 2017;127:2007-2018.
21. Feng S, Wu Z-X, Zhao Z, et al. Engineering of bone- and CD44-dual-targeting redox-sensitive liposomes for the treatment of orthotopic osteosarcoma. *ACS Appl Mater Interfaces*. 2019;11:7357-7368.
22. Lo JH, Hao L, Muzumdar MD, et al. iRGD-guided tumor-penetrating nanocomplexes for therapeutic siRNA delivery to pancreatic cancer. *Mol Cancer Ther*. 2018;17:2377-2388.
23. Sugahara KN, Teesalu T, Karmali PP, et al. Coadministration of a tumor-penetrating peptide enhances the efficacy of cancer drugs. *Science*. 2010;328:1031-1035.
24. Chen H, Sha H, Zhang L, et al. Lipid insertion enables targeted functionalization of paclitaxel-loaded erythrocyte membrane nanosystem by tumor-penetrating bispecific recombinant protein. *Int J Nanomedicine*. 2018;13:5347-5359.
25. Teesalu T, Sugahara KN, Ruoslahti E. Tumor-penetrating peptides. *Front Oncol*. 2013;3:216.
26. Kim MS, Lee E-J, Kim J-W, et al. Gold nanoparticles enhance antitumor effect of radiotherapy to hypoxic tumor. *Radiat Oncol J*. 2016;34:230-238.
27. Ma S, Zhou J, Zhang Y, et al. An oxygen self-sufficient fluorinated nanoplatform for relieved tumor hypoxia and enhanced photodynamic therapy of cancers. *ACS Appl Mater Interfaces*. 2019;11:7731-7742.
28. Hu C, Yang X, Liu R, et al. Coadministration of iRGD with multistage responsive nanoparticles enhanced tumor targeting and penetration abilities for breast cancer therapy. *ACS Appl Mater Interfaces*. 2018;10:22571-22579.
29. Simón-Gracia L, Hunt H, Scodeller P, et al. iRGD peptide conjugation potentiates intraperitoneal tumor delivery of paclitaxel with polymersomes. *Biomaterials*. 2016;104:247-257.
30. Meng F, Speyer CL, et al. PDGFRα and β play critical roles in mediating Foxq1-driven breast cancer stemness and chemoresistance. *Cancer Res*. 2015;75(3):584-593.
31. Inci ID, Tekin V, Kilcar AY, et al. Radioiodination of pimonidazole as a novel theranostic hypoxia probe. *Curr Radiopharm*. 2021;14:46-50.
32. Ding N, Zou Z, Sha H, et al. iRGD synergizes with PD-1 knockout immunotherapy by enhancing lymphocyte infiltration in gastric cancer. *Nat Commun*. 2019;10:1336.

33. Chandna S, Dwarakanath BS, Khaitan D, Mathew TL, Jain V. Low-dose radiation hypersensitivity in human tumor cell lines: effects of cell-cell contact and nutritional deprivation. *Radiat Res.* 2002;157:516-525.

34. Wang H, Najibi AJ, Sobral MC, et al. Biomaterial-based scaffold for in situ chemo-immunotherapy to treat poorly immunogenic tumors. *Nat Commun.* 2020;11:5696.

35. Jiang X, Wang C, Fitch S, Yang F. Targeting tumor hypoxia using nanoparticle-engineered CXCR4-overexpressing adipose-derived stem cells. *Theranostics.* 2018;8:1350-1360.

36. He Z, Yuan J, Shen F, et al. Atorvastatin enhances effects of radiotherapy on prostate cancer cells and xenograft tumor mice through triggering interaction between Bcl-2 and MSH2. *Med Sci Monit.* 2020;26:e923560.

37. Stokes AM, Hart CP, Quarles CC. Hypoxia imaging with PET correlates with antitumor activity of the hypoxia-activated prodrug evofosfamide (TH-302) in rodent glioma models. *Tomography.* 2016;2:9.

38. Hurtado de Mendoza T, Mose ES, Botta GP, et al. Tumor-penetrating therapy for beta5 integrin-rich pancreas cancer. *Nat Commun.* 2021;12:1541.

39. Mao X, Liu J, Gong Z, et al. iRGD-conjugated DSPE-PEG2000 nanomicelles for targeted delivery of salinomycin for treatment of both liver cancer cells and cancer stem cells. *Nanomedicine.* 2015;10:2677-2695.

40. Sugahara KN, Braun GB, de Mendoza TH, et al. Tumor-penetrating iRGD peptide inhibits metastasis. *Mol Cancer Ther.* 2015;14:120-128.

41. Hamilton AM, Aidoudi-Ahmed S, Sharma S, et al. Nanoparticles coated with the tumor-penetrating peptide iRGD reduce experimental breast cancer metastasis in the brain. *J Mol Med (Berl).* 2015;93:991-1001.

42. Pang H-B, Braun GB, Friman T, et al. An endocytosis pathway initiated through neuropilin-1 and regulated by nutrient availability. *Nat Commun.* 2014;5:4904.

43. Begg AC, Stewart FA, Vens C. Strategies to improve radiotherapy with targeted drugs. *Nat Rev Cancer.* 2011;11:239-253.

## SUPPORTING INFORMATION

Additional supporting information may be found in the online version of the article at the publisher's website.